EUROPEAN ORGANIZATION FOR NUCLEAR RESEARCH

ATLAS Internal Note
LARG-NO-025
22 September 1995

THE DESIGN OF ENDCAP EM CALORIMETER WITH CONSTANT THICKNESS OF THE ABSORBER PLATES

S.G.Klimenko, Yu.A.Tikhonov
Budker Institute of Nuclear Physics, Novosibirsk, Russia
A.I.Chekhtman [1)]
Centre de Physique des Particles de Marseille, France

Abstract

The alternative design of the endcap EM calorimeter for Atlas detector is described. In comparison with the TP [2)] design where the absorber plates with a variable thickness are used, the described calorimeter has a constant thickness of the absorber plates. New design of the absorbers allows one to obtain more simple and more uniform endcap calorimeter.

[1)] at the present time is working for BINP, Novosibirsk, Russia
[2)] Technical Proposal

1 Introduction

One of the general ideas developed and tested by the RD3 collaboration is to use the fan-like geometry for the endcap calorimeter of Atlas detector [1, 2]. Compared to the barrel EM calorimeter the fan calorimeter in the endcap has the additional nonuniformity in the η (rapidity) direction. Because of the opening liquid gap the calorimeter response depends on η.

The possible solution of this problem and the detailed description of the fan geometry are given in the ATLAS note [3]. Lets consider the design described in this note as a baseline (or TP) design of the endcap calorimeter.

Two main ideas are used in the baseline design to obtain the calorimeter's uniformity in the η direction:

- To keep the sampling ratio ϵ independent on η,

$$\epsilon = E_a/(E_a + E_p), \tag{1}$$

  where E_a and E_p are the energy deposition in the active (LAr) and passive materials respectively.
- To compensate the signal nonuniformity on η by the distributed high voltage.

The first point implies that the absorber plates have a variable thickness that creates problems for the plates production and makes the calorimeter more expensive.

Unfortunately, the constant sampling ratio itself doesn't guaranty the uniformity of the calorimeter. The signal depends on the rapidity if even ϵ is constant: [1)]

$$Signal \sim \frac{\epsilon}{T_d} = \frac{\epsilon}{g} \cdot V_d, \tag{2}$$

where g is a liquid gap thickness, T_d and V_d are a drift time and drift velocity of free electrons in the liquid. To compensate the effect of the gap variation V_d should be a linear function of g. For a liquid argon the drift velocity is proportional to $E^{0.3}$ [4], where E is an electric field in the gap. Because of the saturation of the drift velocity on E the variation of the electric field is too big ($3 - 15\ kV/cm$). The maximum value of high potential is approximately $3.5\ kV$, that decrease the reliability of the calorimeter. Besides this, because of the limited granularity of the calorimeter, the compensation is not local. If even each cell will have the unique value of the high potential, the signal will be different depending on the point of energy deposition inside the cell (the "remaining nonuniformity"). This effect can introduce the additional constant term in the energy resolution.

In this paper we propose the alternative (or A) design of the calorimeter which is free of the problems described above. The main feature of the alternative design is the constant thickness of the absorber plates. The general design of the calorimeter, the η and ϕ uniformity, the energy resolution - these and other questions are the subject of this paper. Many results obtained for the alternative design are shown in the comparison with ones for the baseline design.

2 The general design of the calorimeter

Some of the calorimeter's parameters, like the position and dimensions of the volume where the active part should be fitted, are determined by the general layout of ATLAS detector [5]. The general parameters which we used in the calculations are shown in table 1.

The active part of the calorimeter consists of the accordion shaped absorber and kapton plates. The gaps between plates are filled with a liquid argon. As in the barrel, the absorbers are made of lead sheets clad between two layers of 0.2 mm thick stainless steel. The thickness of the absorber plates is the same for inner and outer wheels. Table 2 shows the list of materials which are implied to be used for the plate production.

[1)] assuming the infinite lifetime of ionisation and short shaping time τ ($\tau << T_d$).

Table 1: General parameters of the endcap calorimeter.

Z_0	362.3 *cm*	beginning of active part in the Z direction
L	51.0 *cm*	length of active part in the Z direction
	203.6 *cm*	outer radius of the calorimeter
	29.0 *cm*	inner radius of the calorimeter
n	768/384	number of absorbers for outer/inner wheels
k	256/128	number of ϕ-cells for outer/inner wheels
	$1.4 < \eta < 2.4$	rapidity coverage for outer wheel
	$2.4 < \eta < 3.2$	rapidity coverage for inner wheel

Table 2: List of materials: t,w - the layer's thickness and weight for each material, w_{tot} - total weight of each material.

unit cell	material	t, mm	inner wheel		outer wheel	
			w, kg	w_{tot}, t	w, kg	w_{tot}, t
absorber	lead	1.60	5.312	2.040	18.887	14.505
plate	inox	0.40	.921	.354	3.274	2.515
	prepreg	0.30	.125	.048	.443	.340
signal	copper	0.06	.157	.060	.559	.429
plate	kapton	0.24	.100	.038	.354	.272
gap	argon			.495		5.266

The fan-like accordion geometry is described by the following parameters (fig. 1): opening angle (α), zig-zag length, height and step (S,h,d). The parameters S and h are the functions of α:

$$S(\alpha) = \frac{d}{sin\ \frac{\alpha}{2}} - \frac{2\rho}{tg\ \frac{\alpha}{2}} + (\pi - \alpha)\rho, \tag{3}$$

$$h(\alpha) = \frac{d}{tg\ \frac{\alpha}{2}} - \frac{2\rho}{sin\ \frac{\alpha}{2}} + 2\rho, \tag{4}$$

where ρ is the average radius of a fold region. Because of the technological limitations the zig-zag length should be a linear function of the radius. This condition gives the relation between r (or η) and α:

$$S(\alpha) = \frac{\theta}{2m} \cdot (r + r_0), \tag{5}$$

where $2m$ is the number of zig-zag steps (d=L/2m), θ and r_0 are the parameters of a plate before bending (fig. 2, tab.3). The geometry parameters as functions of r (η) are shown in figure 3.

Table 3: The plate's parameters θ and r_0 for inner and outer wheels.

wheel	θ, deg.	r_0, cm
inner	46.0	41.5
outer	17.0	127.3

The total thickness of the active part of the calorimeter X_{tot} is shown in figure 4. The calorimeter has a reasonable thickness for low rapidity events (X_{tot}=24.3X_0 for η=1.46) and the thickness increases with rapidity. It allows to have an optimal amount of dead material in the calorimeter. The total weight of lead for each endcap is 16.5 tons compared to 27.5 tons for the baseline design. For events with $\eta > 1.45$ the thickness is enough to absorb the electromagnetic showers without the visible deterioration of energy resolution because of the backward leakage.

For the rapidity gap $1.40 < \eta < 1.45$ the thickness is less then $24X_0$, but this region is covered by both barrel and endcap calorimeters.

3 η-uniformity

The uniformity in the η direction is considered for the geometry described above. Because of the constant lead thickness and opening gap the sampling ratio is a function of the rapidity. It is easy to show that the sampling ratio is approximately proportional to g (see eq.1) and the ratio ϵ/g should be almost independent on η. The results obtained for ϵ, g, ϵ/g by the analytic calculation [2)] and GEANT (MC) simulation [3)] are shown in figure 5. Indeed the ratio ϵ/g (fig. 5c) is very close to constant. It means that the calorimeter response is compensated and the compensation is local. If the constant high voltage is applied the remaining η-nonuniformity (fig. 5d) arises mainly from the dependence of the drift velocity on the gap:

$$V_d \sim (U/g)^{0.3}. \tag{6}$$

For the alternative design as well as for the baseline design the correction of the signal by the distributed high voltage is necessary. The signal is almost uniform if the value of electric field in the gap is constant. To obtain an ideal uniformity of the calorimeter the distributed high voltage and electric field which are shown in figure 6 have to be applied. For real calorimeter the average value of electric field can be different from one shown in figure 6a. To obtain a correct value of electric field other important effects (electronics noise, pileup noise, etc.) should be taken in to account.

It should be mentioned that for the TP design the calorimeter is not quite uniform if even the distributed high voltage (fig. 6b) is applied. The calorimeter is devided into three parts on the rapidity: $\eta < 1.6$, $1.6 < \eta < 2.4$ and $\eta > 2.4$. Really the signal is uniform only inside each part. For example, the responses of the internal ($\eta > 2.4$) and external ($1.6 < \eta < 2.4$) wheels are different by a factor of 12%.

4 ϕ-uniformity

Due to the fold regions in the accordion structure the total amount of dead material crossed by a particle depends on ϕ that cause the variation of the signal (ϕ-modulation) [6]. The ϕ-modulation depends on the arrangement of the plates in the accordion structure which, in the case of fan-like geometry, can be described by a "defect of alignment":

$$\Delta_a = \frac{1}{a}(h + a - \frac{2\pi r}{k}), \tag{7}$$

where a is a thickness of absorber plate. The defect of alignment shows the overlapping of the fold regions of the absorber plates (see fig. 1). The parameters of the accordion structure (n, m, k, θ, r_0, etc.) have to be chosen to provide an optimal value and as small as possible variation of Δ_a on η.

The ϕ-modulation was checked using the particles with minimal ionization. The best ϕ-modulation was obtained by minimization of the integral ϕ-uniformity which is determined as

$$\Phi_I = \frac{(\overline{s^2} - \overline{s}^2)^{\frac{1}{2}}}{\overline{s}}, \tag{8}$$

where $\overline{s}$ and $\overline{s^2}$ are mean and mean square values of the signal calculated over the unit cell. The best integral ϕ-uniformity was obtained if the defect of alignment is $\sim 50\%$.

[2)] will be published

[3)] produced on BASTA claster at CCPN (Lyon)

Unfortunately, it isn't possible to provide the optimal value of the defect of alignment and hence a good ϕ-uniformity in the full η region covered by the calorimeter. For the rapidity range $1.6 < \eta < 3.0$ the calorimeter is rather uniform (fig. 7), but outside this range the defect of alignment is not optimal (the same situation is for the TP design too).

Figure 8 shows the examples of the ϕ-modulation for MIP in the unit cell. The ϕ-modulation for EM showers is much less (fig. 9). It was obtained using the GEANT simulation of the showers (100GeV electrons) in the calorimeter. As for the barrel calorimeter, the ϕ-modulation can be corrected. We used the following formula to fit the MC data:

$$Signal(\phi) = p_1 \cdot (1 + p_2 \cdot cos(\phi) + p_3 \cdot exp(-\frac{1}{2}(\frac{\phi}{p_4})^2), \quad (9)$$

where, p_1, p_2, p_3, p_4 are the fitting parameters. The value of ϕ-modulation is determened by two parameters: p_2 - *cos*-term, p_3 - *exp*-term. This parameters were used to estimate the ϕ-uniformity of the calorimeter. For the rapidity range $1.6 < \eta < 3.0$ the typical value of the ϕ-modulation is $\pm 1\%$ and it is approximately the same for A and TP designs (tab.4).

Table 4: ϕ-modulation for showers (100 GeV electrons): p_2 - *cos*-term, p_3 - *exp*-term.

	A design		TP design	
η	$\pm p_2, \%$	$p_3, \%$	$\pm p_2, \%$	$p_3, \%$
1.6	0.76	1.86	0.98	4.20
1.8	1.07	0.01	1.07	0.48
2.0	1.09	0.22	1.04	0.01
2.2	0.91	0.85	0.70	0.31
2.6	1.15	1.10	1.32	0.04
2.8	1.01	1.39	0.93	0.46
3.0	0.82	3.91	0.84	2.91

5 Energy resolution

There are many factors which affect the energy resolution of a real calorimeter. In this paper only two of them are discussed: the sampling fluctuations and the constant term of the energy resolution.

To estimate the energy resolution we simulated EM showers from 100 GeV electrons going through the calorimeter. No any dead materials were in front of the accordion structure. The calorimeter's response was corrected for ϕ-modulation. Histogram in figure 10 shows a typical amplitude (ϵ/g) distribution obtained in the GEANT simulation. The energy resolution as a function of η is shown in figure 11.

To select the sampling term we normalized the calorimeter response to the total energy deposition in the accordion structure. In figure 12 the sampling term as a function of the rapidity is shown . For comparison the energy resolution obtained for the TP design is shown on the same plot. There is no significant difference in the sampling term between two versions of the calorimeter. Figure 13 shows the resolution of the calorimeter for the transverse energy (E_T). The dependence of the E_T resolution on η is quite uniform.

Concerning the constant term the alternative design has better performances compared to the baseline design. Because of the local compensation of the signal the remaining nonuniformity is considerably less. We estimated the constant term for both options of the calorimeter using the MC simulation (tab.4). The value σ_0 gives the energy resolution when the calorimeter response is almost uniform (the simulated signal is proportional to ϵ or ϵ/g for the baseline or alternative designs respectively). If the simulated signal is proportional to $\epsilon/g^{1.3}$ (U=constant) the

η-nonuniformity gives the maximum contribution to the energy resolution (σ_U). The constant term σ_c is estimated as

$$\sigma_c = \sqrt{\sigma_U^2 - \sigma_0^2}. \tag{10}$$

For the alternative design the average constant term ($1.6 < \eta < 2.2$) is consistent with zero but

Table 5: The sampling and constant terms for two versions of the calorimeter.

	A design			TP design		
η	$\sigma_0, \%$	$\sigma_U, \%$	$\sigma_c^2, \%^2$	$\sigma_0, \%$	$\sigma_U, \%$	$\sigma_c^2, \%^2$
1.6	7.2	7.4	0.04	8.3	9.6	0.23
1.8	7.3	7.3	0.01	7.0	8.3	0.20
2.0	7.9	7.7	-0.04	7.6	8.3	0.11
2.2	8.0	7.9	-0.01	7.8	8.6	0.13
1.6-2.2	$\sigma_c^2 = 0.00 \pm 0.02$			$\sigma_c^2 = 0.17 \pm 0.03$		

for the baseline design σ_c is approximately 0.4%.

6 Conclusion

There are no significant differences between the baseline and alternative designs except the difference in the design of the absorber plates. The main idea (fan-like geometry), the design of cryostat, the total sizes - all are the same as for the baseline design. The performances of the calorimeter are also the same or better:

- The mechanics problems are much easier. The absorber plates can be made with better tolerances that leads to less constant term in the energy resolution.
- The uniformity of the signal in η direction is better. The calorimeter response is intrinsically compensated. The signal is almost independent on η if the applied electric field is constant. The partial local compensation of the signal provides:
  - less constant term,
  - less variation of the electric field and smaller high voltage, that increase the reliability of the calorimeter.
- The ϕ-uniformity of the calorimeter is the same as one for the baseline design.
- The sampling term of the energy resolution is almost the same as one for the baseline design.
- The total thickness of the calorimeter has a proper dependence on the rapidity - the calorimeter thickness increases with rapidity.
  - That is better for absorption of the high energy showers for the large rapidity events.
  - It provides the uniform transverse energy resolution.
  - The total weight of the calorimeter is considerably less: 22 tons for each endcap compared to 31 tons for the baseline design.

7 Acknowledgments

We would like to express our gratitude to Peter Jenni and Daniel Fournier for the support and Sylvain Tisserant for given possibility to use the BASTA claster at CCPN for the simulation.

References

[1] B.Aubert et al. (RD3 collaboration) Status report and further R&D for EM and hadron calorimetry. CERN/DRDC/93-4.

[2] ATLAS. Letter of intent for a General purpose pp experiment at the Large Hadron Collider at CERN. CERN/LHCC/92-4.

[3] A.Chekhtman, D.Fouchez, E.Monnier. The accordion in the endcap: geometry and characteristics. ATLAS internal note LARG-NO-4(1994).

[4] M.Coux. Etudes des hautes tensions sur le calorimetre de type "spanish fan". Rapport de stage au CERN (23/3/93-23/6/93). Universite Joseph Fourier, D.E.A. Methodes Physique Experimentales. Responsable de stage: V.Vuillemin, P.Petroff.

[5] ATLAS. Technical Proposal for a General Purpose pp experiment at the Large Hadron Collider at CERN. CERN/LHCC/94-13.

[6] B.Aubert et al. (RD3 collaboration). Performance of a Liquid Argon Accordion Calorimeter with Fast Readout. Nucl. Instr. & Meth. vol. A321(1992) p.467-478.

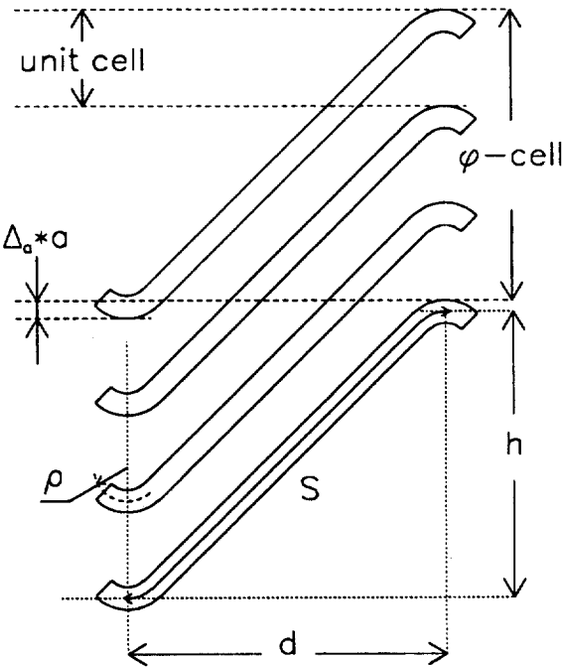

Figure 1: The lay-out of accordion absorbers.

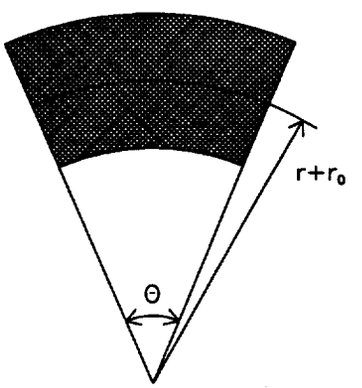

Figure 2: The shape of a plate before bending for nonprojective gap between two wheels.

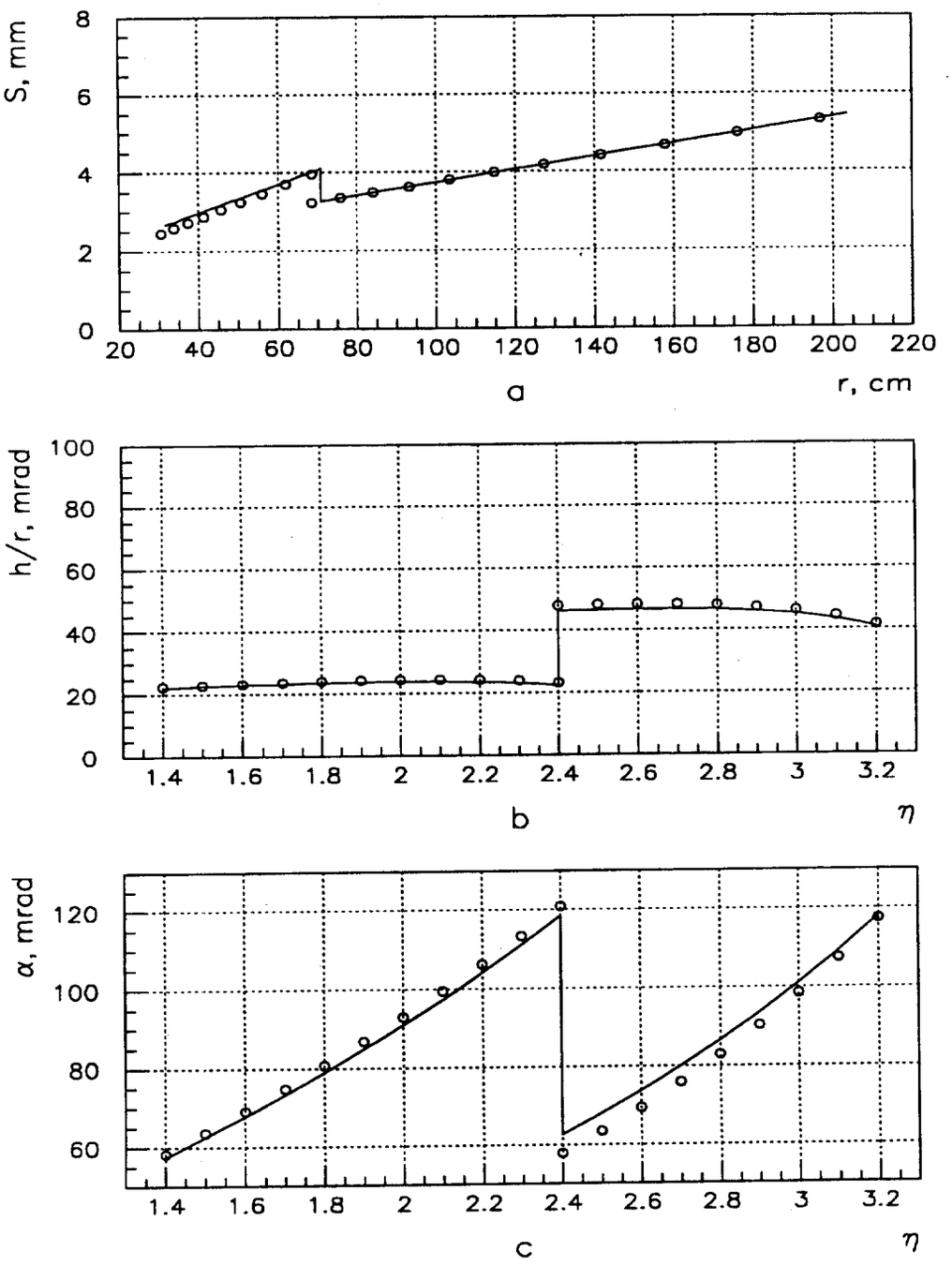

Figure 3: The geometry parameters as functions of r or η: a) - zig-zag length, b) - zig-zag height divided by radius, c) - opening angle: — - A design, o - TP design.

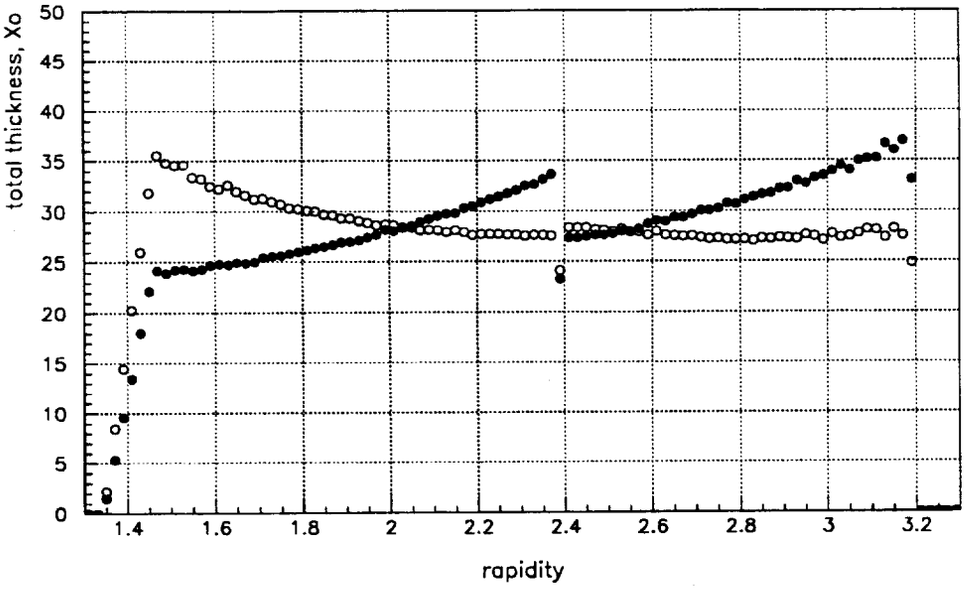

Figure 4: Total thickness of the calorimeter (in terms of radiation lengths) obtained by GEANTINO scan: —, • - A design, ○ - TP design.

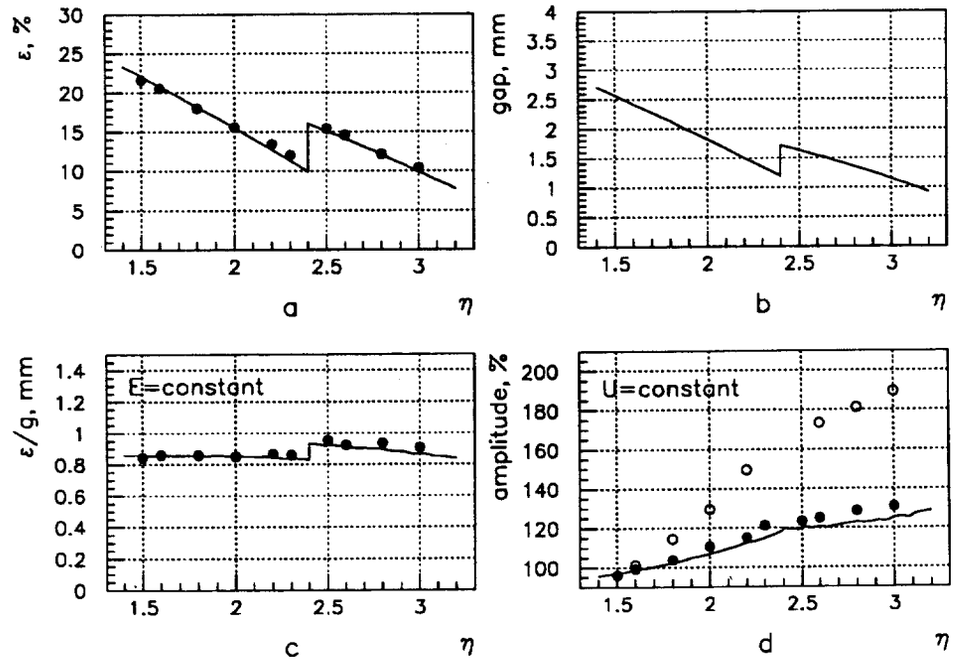

Figure 5: The parameters which determine the uniformity of the calorimeter as functions of η: a) - ϵ, b) - g, c) - ϵ/g, d) - amplitude of the signal for constant high voltage applied. — - analytic calculation for A design, • - MC simulation for A design, ○ - MC simulation for TP design.

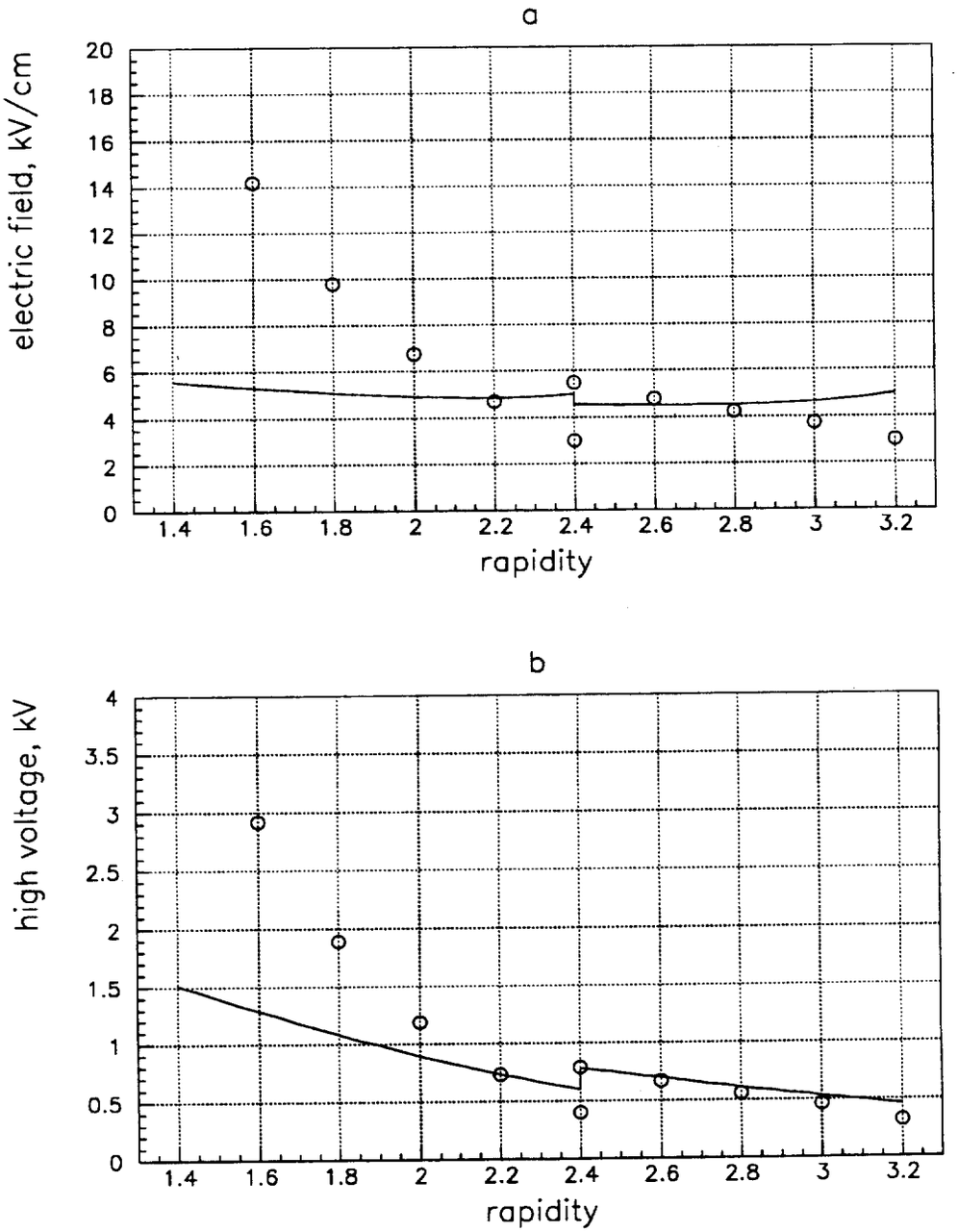

Figure 6: The electric field (a) and high voltage (b) as functions of η: — - for A design, o - for TP design.

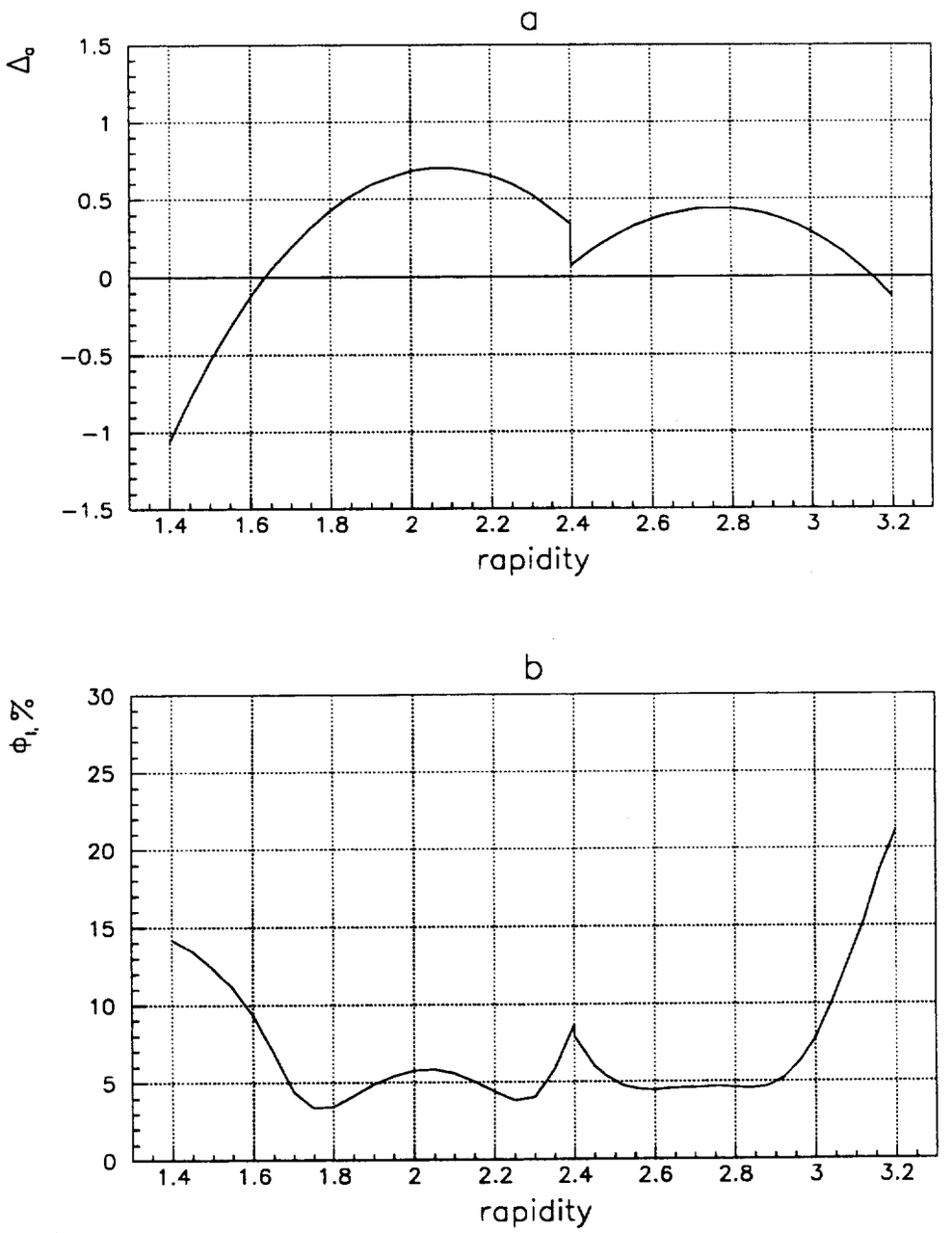

Figure 7: The defect of alignment Δ_α (a) and integral ϕ-uniformity for MIP Φ_I (b) as functions of η.

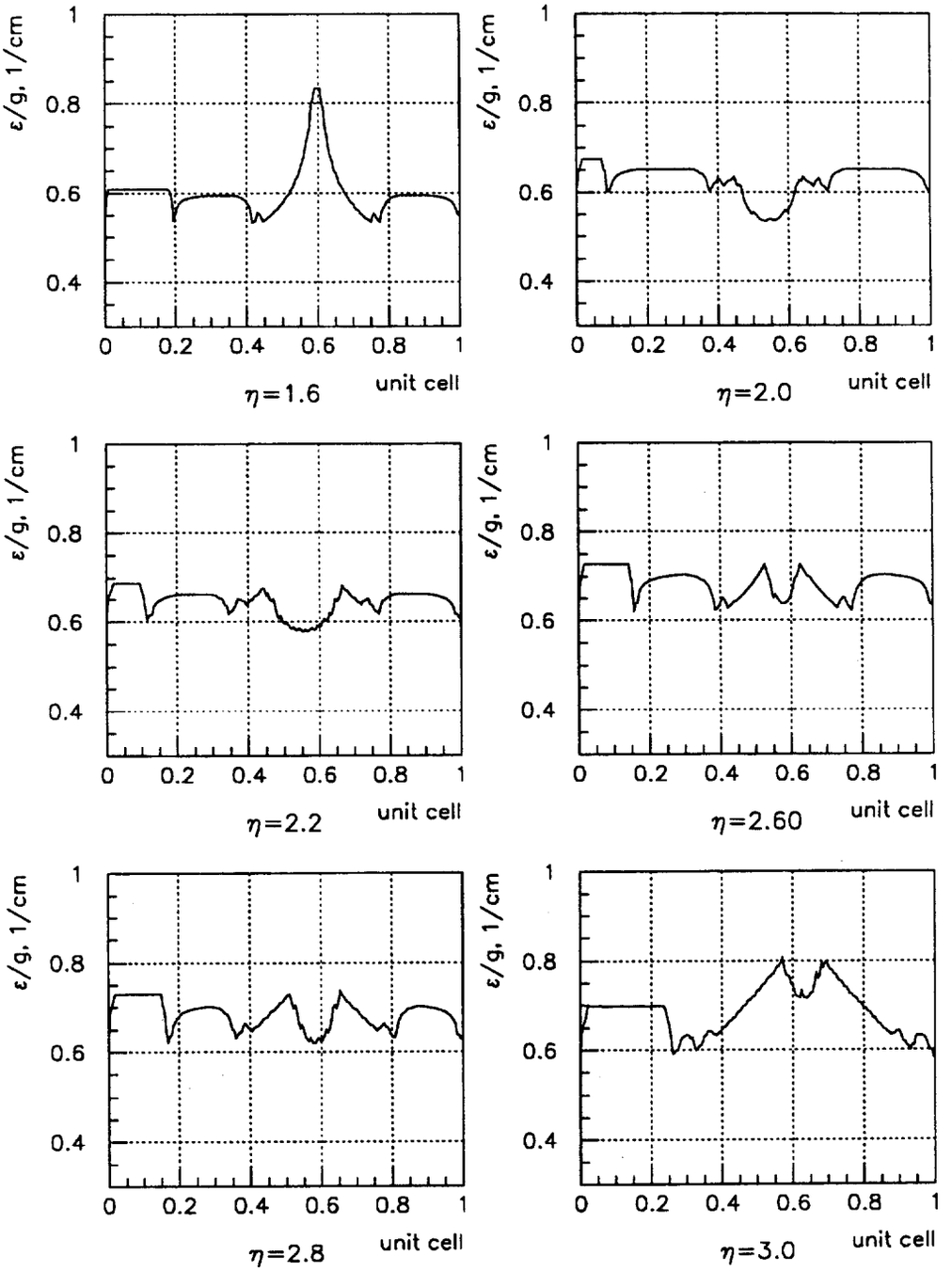

Figure 8: The signal uniformity for MIP in the unit cell.

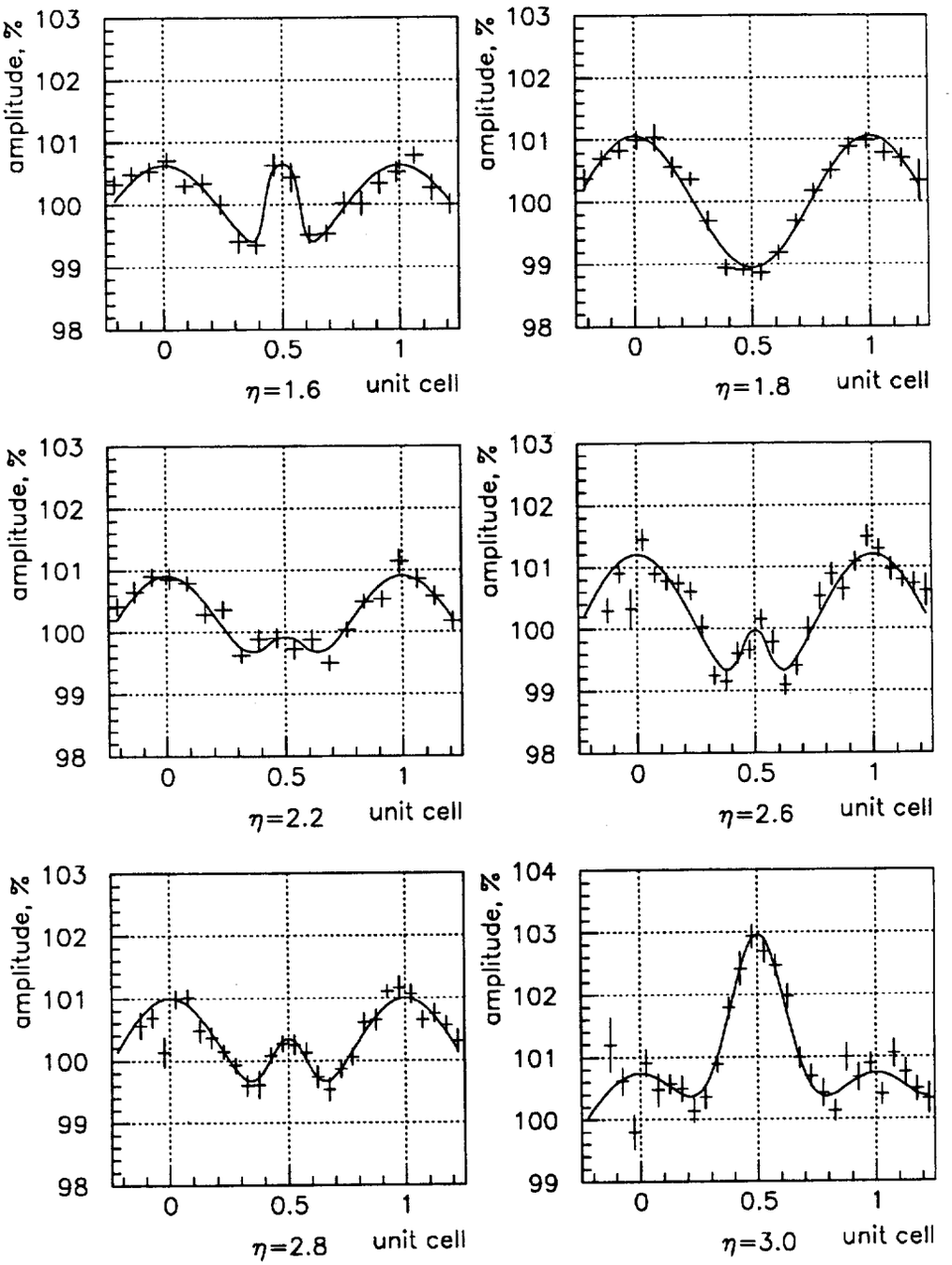

Figure 9: The signal uniformity for showers (100 GeV electrons) in the unit cell: + - MC data, — - fit.

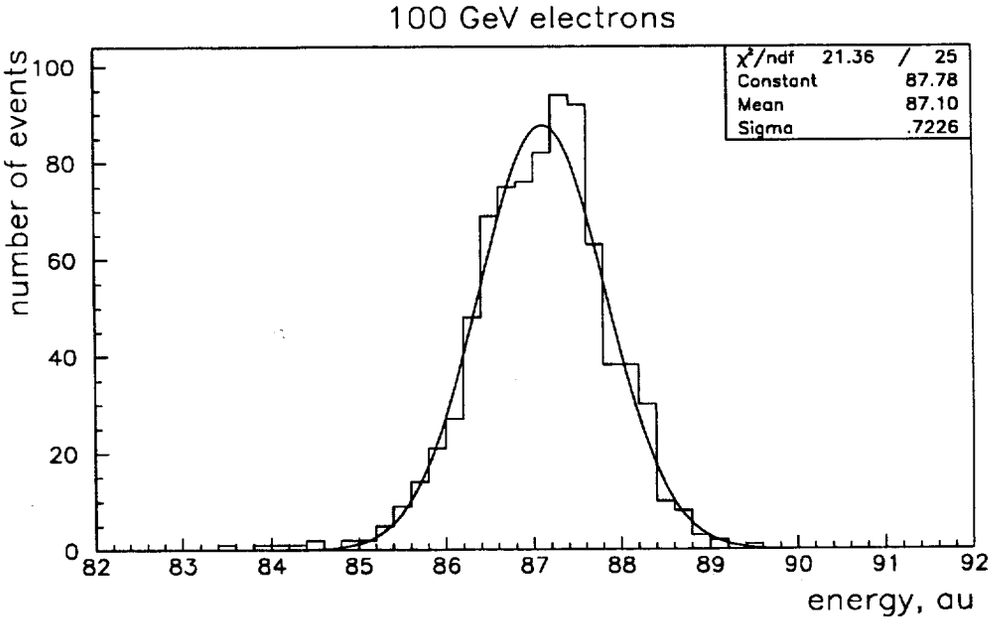

Figure 10: The example of amplitude distribution obtained in the GEANT simulation.

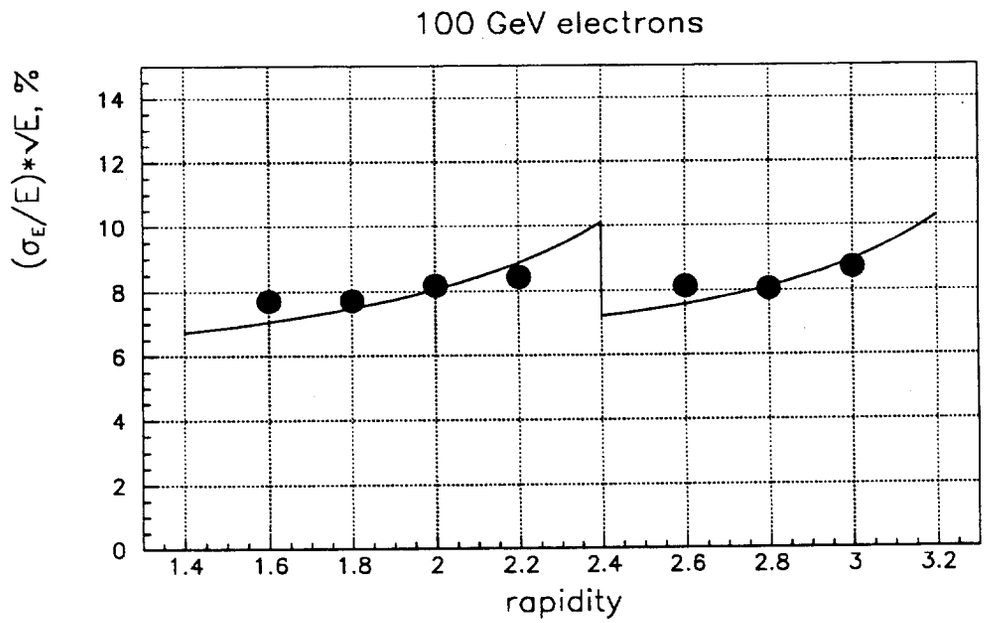

Figure 11: Energy resolution of the calorimeter: — - analytic calculation for A design, • - MC simulation for A design.

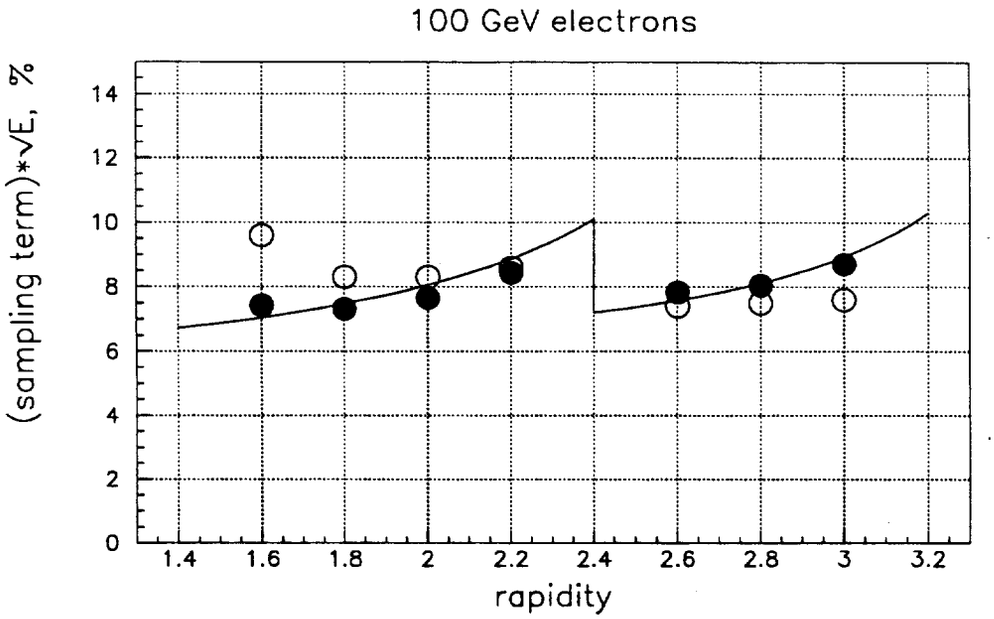

Figure 12: Energy resolution of the calorimeter with leakage correction (sampling term): — - analytic calculation for A design, • - MC simulation for A design, ○ - MC simulation for TP design.

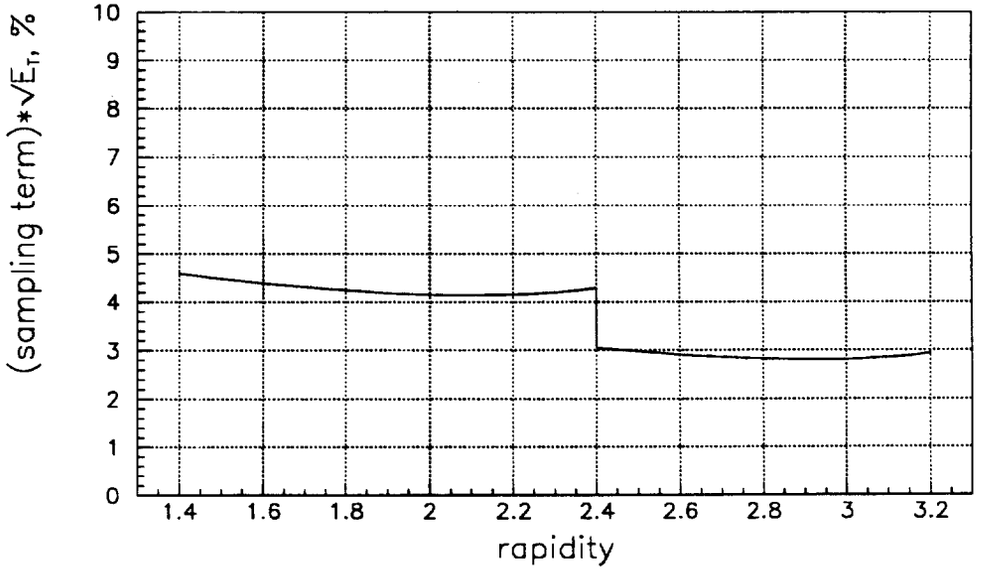

Figure 13: Transvers energy resolution of the calorimeter: — - analytic calculation for A design.